# Log-normality of temperature dissipation in a turbulent boundary layer

R. A. Antonia and K. R. Sreenivasan

*Department of Mechanical Engineering, University of Newcastle, New South Wales, 2308, Australia*
(Received 7 February 1977; final manuscript received 2 May 1977)

Using measurements of all three components of the temperature dissipation $\chi$ in a laboratory boundary layer, the measured probability density $p(\chi_r)$ of $\chi_r$, or $\chi$ averaged over a distance $r$, is found to be closely log-normal over a significant range of $r$. The variance $\sigma^2$ of $\ln\chi_r$ follows the relation $\sigma^2 = A + \mu\ln(L/r)$, with $\mu = 0.35$, where $L$ is an integral scale of turbulence. High order moments, up to order 5, of $\chi_r$ show a power-law variation with $r/L$. With increasing order of the moment, the power-law exponents become increasingly smaller than the corresponding values implied by assumed log-normality of $p(\chi_r)$ but are consistent with the bounds given by Novikov's theory. It is suggested that the observed close agreement with log-normality of $p(\chi_r)$ may be misleading when sufficiently high order moments of $\chi_r$ are considered.

## INTRODUCTION

In their treatment of the refined similarity hypothesis which takes into account fluctuations of the dissipation field, Kolmogoroff[1] and Obukhov[2] have suggested that the probability density of $\epsilon_r$, the dissipation averaged over a sphere of radius $r$ ($r \ll L$), is log-normal. They also assumed that the variance $\sigma^2$ of $\ln\epsilon_r$ may be given by

$$\sigma^2 = A + \mu \ln(L/r) , \qquad (1)$$

where $\mu$ is presumably a universal constant, $L$ is an integral scale of turbulence, and $A$ is a constant that may depend on the macrostructure of the flow. The two previous assumptions taken together have, for convenience, sometimes been referred to as Kolmogoroff's third hypothesis. Yaglom[3] and Gurvich and Yaglom[4] have given heuristic arguments in support of the third hypothesis. These arguments have also been extended to scalar fields (such as temperature concentration) or indeed any positive-definite quantity associated with the small scale structure of turbulence. The experimental verification of this hypothesis is important since measured properties of small scale turbulence, such as high order moments of derivatives of velocity and temperature fluctuations or high order moments of structure functions of velocity and temperature, are usually compared with predictions of the hypothesis.

In a previous paper,[5] all three components of the fluctuating temperature dissipation $\chi$ were measured simultaneously in the inner region of a fully developed turbulent boundary layer at moderate laboratory Reynolds numbers. The probability density of $\chi$ or $\chi_r$, the average of $\chi$ over a distance $r$, was found to be more closely (although not exactly) log-normal than the probability densities of the individual components. This result supported the suggestion by Gibson and Masiello[6] that the log-normality of $p(\chi_r)$ excludes the possibility of log-normal distributions for the individual components and vice versa. It was also found[5] that assumption (1) was valid for $\chi_r$ over a fairly large range of $r$ (in excess of a decade). In this paper, we present further results on the statistics of $\chi_r$ or $\ln\chi_r$ with a view to testing the implications of (1) and the log-normality of $\chi_r$ with regard to the high order moments of $\chi_r$. Calculated high order moments $\overline{\chi_r^n}$ of $\chi_r$ show a power-law dependence on $(L/r)$, consistent with both Novikov's[7] theory and the deductions from Kolmogoroff's third hypothesis. However, the exponents of the power-law are significantly smaller (for $n \geq 3$) than those suggested by the third hypothesis, and are within the bounds suggested by Novikov.[7]

## EXPERIMENTAL PROCEDURES

All three components of the temperature dissipation were measured with a four-wire probe (described in Ref. 5), with each wire sensitive to temperature fluctuation only. Instantaneous gradients of temperature $\partial\theta/\partial y$ and $\partial\theta/\partial z$ in directions normal and transverse to the wall, respectively, were obtained from the approximate relations

$$\partial\theta/\partial y \simeq \Delta\theta/\Delta y, \quad \partial\theta/\partial z \simeq \Delta\theta/\Delta z ,$$

where $\Delta y$ and $\Delta z$ are the separations, in the $y$ and $z$ directions, respectively, between pairs of parallel wires of the four-wire probe. The values of $\Delta y$ and $\Delta z$ were approximately equal to six times the Kolmogoroff length scale $\eta$. The validity of these approximations is ascertained in Ref. 5. The streamwise temperature gradient $\partial\theta/\partial x$ was obtained with the use of Taylor's hypothesis from the temporal derivative of the signal from one of the wires. Signals proportional to $\partial\theta/\partial x$, $\partial\theta/\partial y$, $\partial\theta/\partial z$ measured at several points in the inner region of a turbulent boundary layer well downstream of a step change in surface heat flux, were recorded on a Philips ANALOG-7 FM tape recorder at a speed of 76.2 cm/sec. At the measuring station, the velocity boundary layer, which develops with a zero pressure gradient, has a thickness $\delta$ of 8.6 cm while the thermal layer thickness is 6.6 cm. The free stream velocity $U_1$ is 9.45 m/sec and the Reynolds number based on the momentum thickness is 5730.

The tape recorder was played back at a speed of 2.38 cm/sec and signals proportional to $\partial\theta/\partial x$, $\partial\theta/\partial y$, and $\partial\theta/\partial z$ were digitized at a frequency of 630 Hz. This

TABLE I. Turbulence Reynolds number and integral length scale.

| $y/\delta$ | $R_\lambda$ | $L/\delta$ |
|---|---|---|
| 0.06 | 134 | 0.285 |
| 0.12 | 153 | 0.394 |
| 0.18 | 169 | 0.470 |
| 0.24 | 175 | 0.541 |

corresponds to a real time frequency $f_s$ of 20 160 Hz which is somewhat larger than twice the maximum value of the Kolmogoroff frequency at the measurement station. Digital records used to compute statistics of $\chi$ comprised 332 800 characters, equivalent to a real time duration of 16.5 sec. Values of $\chi_\tau$ were determined by averaging $\chi$ over a time interval $\tau$ which ranged from 1 to about 300 digital samples (1 sample is equivalent to $f_s^{-1}$ sec). In the following sections, it is assumed that $\chi_\tau$ is equivalent to $\chi_r$, using one form of Taylor's hypothesis $r = -U\tau$, where $U$ is the local mean velocity. Statistics of $\chi_r$ or $\ln\chi_r$ are presented at four points ($y/\delta = 0.06$, 0.12, 0.18, 0.24) in the fully turbulent part of the layer. In this region, the turbulence Reynolds number $R_\lambda \equiv \overline{u^2}^{1/2}\lambda/\nu$ ($\lambda$ is the Taylor microscale $\overline{u^2}^{1/2}/\overline{(\partial u/\partial x)^2}^{1/2}$, $u$ is the streamwise velocity fluctuation) is in the range 135 to 175. For convenience, it is assumed that the isotropic relation $L/\lambda = R_\lambda/15$ gives a good measure of the integral length scale $L$. Values of $R_\lambda$ and $L$ are given in Table I.

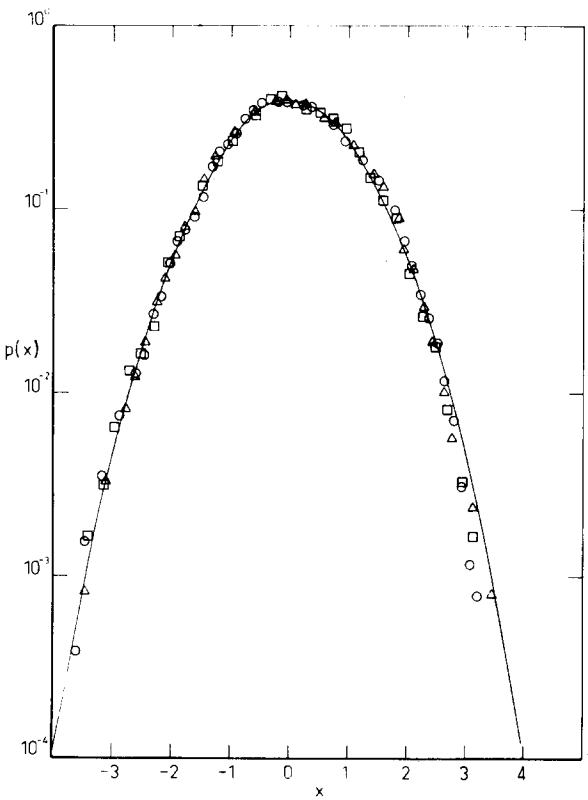


FIG. 1. Probability density function of $x = (\ln\chi_r - \ln\chi_r)/\sigma$ at $y/\delta = 0.12$. ○, $r/L = 0.09$; △, 0.23; □, 0.58. Solid curve is the Gaussian with same mean and variance.

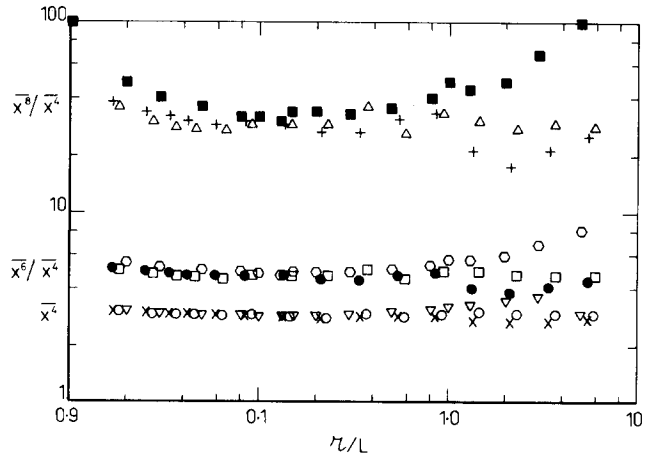


FIG. 2. Normalized fourth, sixth, and eighth order moments of $x$ as a function of averaging length scale $r$. $\overline{x^4}$: ▽, $y/\delta = 0.06$; ○, 0.12; ×, 0.24. $\overline{x^6}/\overline{x^4}$: ○, $y/\delta = 0.06$; □, 0.12; ●, 0.24. $\overline{x^8}/\overline{x^4}$: ■, $y/\delta = 0.06$; △, 0.12; +, 0.24.

## PROBABILITY DENSITY OF $\chi_r$ OR $\ln\chi_r$

The probability density function of $\ln\chi_r$ is shown, in semi-logarithmic coordinates, in Fig. 1 for $y/\delta = 0.12$ and three values of $r/L$ (0.09, 0.23, and 0.58). The probability density $p(x)$ is such that $\int_{-\infty}^{\infty} p(x)\,dx = 1$, where $x = (\ln\chi_r - \overline{\ln\chi_r})/\sigma$, $\overline{\ln\chi_r}$ and $\sigma$ being, respectively, the measured mean and standard deviation of $\ln\chi_r$. For $p$ greater than about 0.01, it is difficult to distinguish departures of the measured $p$ from the Gaussian probability density. Departures are more noticeable for the tails of the measured $p$ and are consistent with the measured negative odd order moments of $x$. The trend of the results in Fig. 1 is also observed at the other values of $y/\delta$ considered here. It should also be noted that the equality $\overline{\ln(\chi_r/\overline{\chi})} = -\sigma^2/2$, implied by log-normality, is very closely satisfied by experimental values of $\overline{\ln\chi_r}$ and $\sigma^2$ for all values of $y/\delta$.

Values of $\overline{x^4}$, the flatness factor of $(\ln\chi_r - \overline{\ln\chi_r})$, are shown in Fig. 2 together with the ratios $\overline{x^6}/\overline{x^4}$ and $\overline{x^8}/\overline{x^4}$. For $r/L \simeq 0.03$, the normalized fourth, sixth, and eighth order moments appear to be in close agreement with the Gaussian values. In the range $0.03 < r/L < 1.0$ the ratios $\overline{x^8}/\overline{x^4}$ and $\overline{x^6}/\overline{x^4}$ are somewhat smaller than the corresponding Gaussian values of 35 and 5, respectively. For $r/L$ near unity, the agreement between even order moments and Gaussian results is again reasonable while odd-order moments (not shown here) are closer to zero than those at $r/L \simeq 0.03$.

The probability density of $\chi_r$ has been derived from the probability density of $\ln\chi_r$ using the relation $p(\chi_r)d\chi_r = p(\ln\chi_r)d(\ln\chi_r)$ and is shown in semi-logarithmic coordinates in Fig. 3 for $r/L = 0.09$, 0.23, and 0.58 at $y/\delta = 0.12$. Also shown for comparison in this figure is the log-normal probability density of $\chi_r$

$$p(\chi_r) = (2\pi)^{-1/2}(\chi_r\sigma)^{-1}\exp[-(\ln\chi_r - \overline{\ln\chi_r})^2/2\sigma^2] \qquad (2)$$

for measured values of the mean and variance of $\ln\chi_r$. In Fig. 3 values of $\chi_r$ have been normalized by the mean dissipation $\overline{\chi}$ (identical to $\overline{\chi_r}$) and the values of $p(\chi_r)$ are

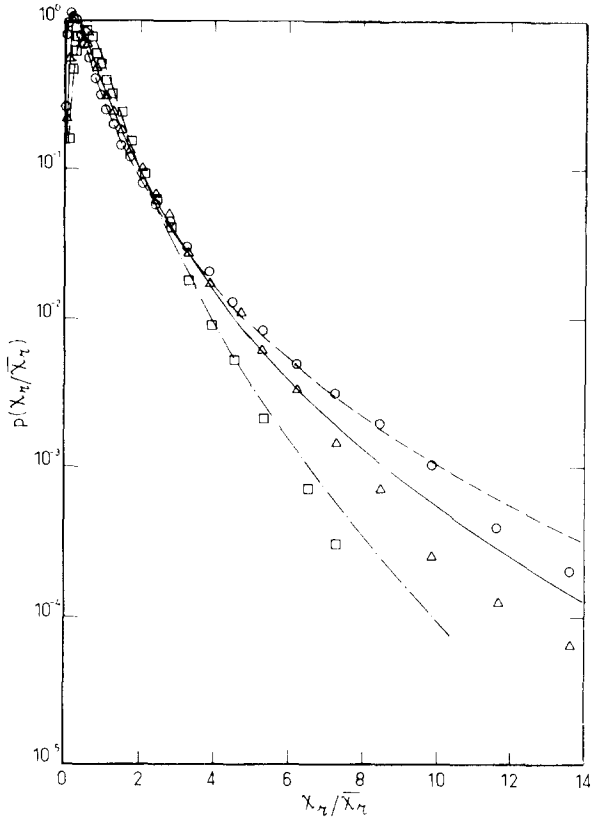

FIG. 3. Probability density function of $\chi_r$ at $y/\delta = 0.12$. o, – – –, $r/L = 0.09$; △, ——, 0.23; —·—·—, □, 0.58. Symbols refer to measured values of $p(\chi_r)$ and curves to log-normal distribution calculated for measured values of $\overline{\ln \chi_r}$ and $\sigma^2$.

such that $\int_0^\infty p(\chi_r)\,d\chi_r = 1$. For all three values of $r/L$, the log-normal density is a good approximation to the measured $p(\chi_r)$ for $\chi_r \gtrsim 0.003$, but is significantly higher in the tail region than the measured values. The maximum value of the calculated $p(\chi_r/\overline{\chi})$ and the value of $\chi_r$ at which it occurs are in good agreement with the log-normal values of $p_{max} = \exp(\sigma^2)/\sigma(2\pi)^{1/2}$ at $\chi_r/\overline{\chi_r} = \exp(-3\sigma^2/2)$.

The variance $\sigma^2$, plotted vs $\ln L/r$ in Fig. 4 for all the four values of $y/\delta$, exhibits a linear portion over a relatively large range of $r/L$ ($0.05 \leq L/r \leq 0.75$). This provides some *a posteriori* justification for the use of the

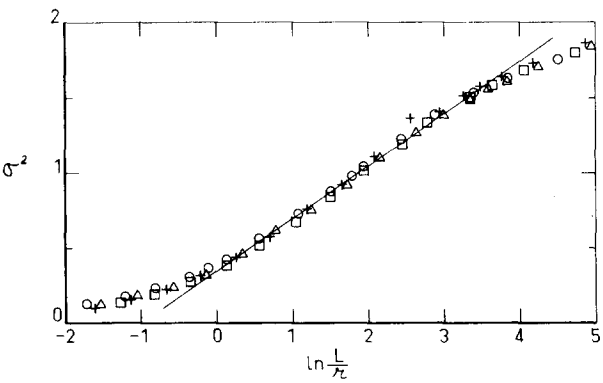

FIG. 4. Variance of $\ln \chi_r$ as a function of $\ln (r/L)$. o, $y/\delta = 0.03$; □, 0.12; +, 0.18; △, 0.24.

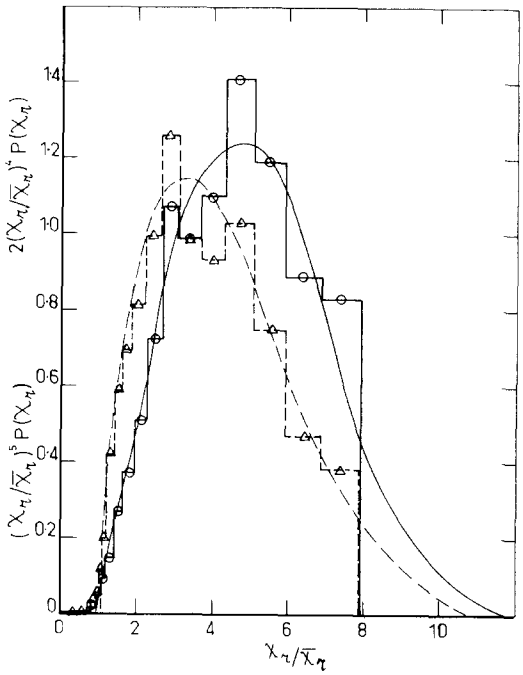

FIG. 5. Fourth and fifth order moments of $\chi_r$ using measured and smoothed values of $p(\chi_r)$. o, $(\chi_r/\overline{\chi_r})^4\, p(\chi_r)$; △, $(\chi_r/\overline{\chi_r})^5\, p(\chi_r)$. $y/\delta = 0.12$, $r/L = 0.58$.

range $0.1 \lesssim r/L \lesssim 0.6$ in Fig. 1, although Kolmogoroff's theory was proposed for $\eta \ll r \ll L$. As discussed in Ref. 5, one of the advantages of using $\chi$ instead of one of its components, is to allow for a more meaningful test of Kolmogoroff's hypothesis in laboratory flows. In this range of $r/L$, values of the constants $A$ and $\mu$ in Eq. (1) are both approximately equal to 0.35. It should be noted here that a different choice for the length scale $L$ would have resulted in a slightly different value of $A$ but would not have affected the good collapse of the data in Fig. 4.

## MOMENTS OF $\chi_r$

High order moments $\overline{\chi_r^n}$ were computed from the probability density of $\chi_r$ with the use of the relation

$$\overline{\chi_r^n} = \int_0^\infty \chi_r^n\, p(\chi_r)\, d\chi_r \,, \tag{3}$$

for values of $n$ ranging from 2 to 5. The integrand in (3) shows good closure at large values of $\chi_r$ for values of $n = 2$ and 3. For $n = 4$ and $n = 5$, moments were obtained by calculating the area under $\chi^n p(\chi)$ using either actual or smoothed values of $p$ (see Fig. 5). Both methods yielded almost identical values for the moments.

The assumption of log-normality for $p(\chi_r)$ leads to moments $\overline{\chi_r^n}$ given by the expression

$$\overline{\chi_r^n} = \overline{\chi}^n \exp(n\,\overline{\ln \chi_r} + \tfrac{1}{2} n^2 \sigma^2) \,. \tag{4}$$

Defining $F^n$ as the ratio $\overline{\chi_r^n}/\overline{\chi}^n$, (4) may be written as

$$F^n = \exp[\tfrac{1}{2} n(n-1)\sigma^2] \,. \tag{5}$$

With $\sigma^2$ given by (1) and using the empirical result $A = \mu$, Eq. (5) may be re-expressed as

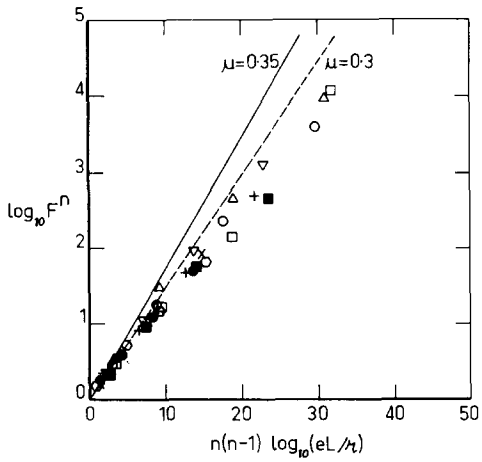


FIG. 6. High order moments of $\chi_r$ obtained for several values of $r/L$ and $y/\delta$. $y/\delta = 0.12$: o, $r/L = 0.09$; +, 0.23; ●, 0.58. $y/\delta = 0.18$: △, $r/L = 0.08$; ▽, 0.19; ×, 0.50. $y/\delta = 0.24$: □, $r/L = 0.07$; ■, 0.18; ○, 0.46. Straight lines correspond to values of $\mu = 0.35$ (——) and 0.30 (— —).

$$\log_{10} F^n = (n/2)(n-1)\log_{10}(eL/r)^{\mu} \tag{6}$$

over a range of $r/L$ for which (1) applies. A plot of experimental values of $\log_{10}F^n$ vs $(n/2)(n-1)\log_{10}(eL/r)$ should yield a universal straight line with a slope given by the value of $\mu$ provided that log-normality of $p(\chi_r)$ is satisfied and that $r$ is chosen to be in the range for which Eq. (1) applied. Experimental values for $F^n$ ($n = 2$ to 5), shown in Fig. 6, lie close to the line of slope $\mu = 0.35$ for $n = 2$ and 3, but deviate appreciably from this line at larger values of $n$. This depature is consistent with the observed depature (Fig. 3) of measured $p(\chi_r)$ from the log-normal probability density. All data points lie relatively close to one another and there is no observable systematic influence of the averaging length $r$ on the trend of the data.

We must emphasize, however, that although Eq. (6) is applied here over an experimental range of $r$ for which Eq. (1) is valid, the condition $\eta \ll r \ll L$ is not rigorously satisfied for the present low $R_\lambda$ data. However, even at these low Reynolds numbers, measured spectral densities of all three temperature gradients are consistent with the concept of local isotropy for fine

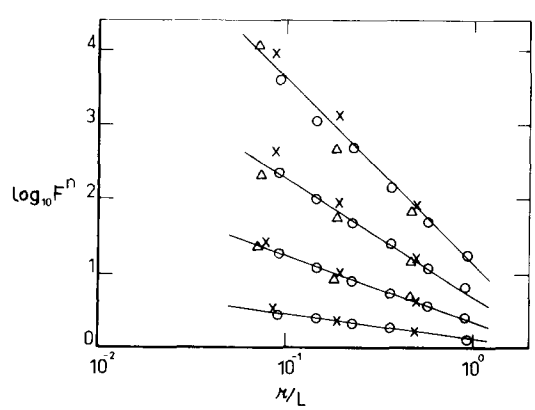


FIG. 7. Power law dependence of $\overline{\chi_r^n}/\overline{\chi_r}^n$ on $r/L$ (from bottom to top) for $n = 2$, 3, 4 and 5. o, $y/\delta = 0.12$; ×, 0.18; △, 0.24.

TABLE II. Values of power-law index $\mu_n$.

| $n$ | Present | Kholmyanskii (Ref. 11) | Novikov (Ref. 7) | Log-normal ($\mu = 0.35$) | Bounds on $\mu_n$ (Novikov Ref. 7) |
|---|---|---|---|---|---|
| 3 | 0.88 | 0.95 | 1.00 | 1.05 | 1.35 |
| 4 | 1.55 | 1.65 | 1.68 | 2.10 | 2.35 |
| 5 | 2.47 | 2.34 | 2.41 | 3.50 | 3.35 |

scale turbulence. While the measured skewness of $\partial\theta/\partial z$ is nearly zero, the measured skewness of $\partial\theta/\partial x$ and of $\partial\theta/\partial y$ is of order unity. It may be argued,[8] however, that the nonzero values of $\overline{(\partial\theta/\partial x)^3}$ and of $\overline{(\partial\theta/\partial y)^3}$, or at least of the former, are not inconsistent with the concept of local isotropy.

It should be noted that a particular form of plotting used in Fig. 6 has been adopted by Frenkiel and Klebanoff[9] who plotted $\log_{10}\{\overline{(\partial u/\partial t)^{2n}}/[\overline{(\partial u/\partial t)^2}]^n\}$ vs $n(n-1)\log_{10}R_\lambda$ for values of $n$ as high as seven. These authors arrived at this method of plotting by considering that $r = \eta$ and assuming that, at very large Reynolds numbers, $A$ in Eq. (1) may be neglected so that $\sigma^2 \propto \ln R_\lambda^{3\mu/2}$. Most of the data used in Ref. 9 was, however, obtained from relatively low Reynolds number grid and boundary layer turbulence, but the atmospheric data ($n = 2$) used in the plot were shown to be consistent with the trend of the laboratory data, a result which appears encouraging for the extrapolation of laboratory data to large values of $R_\lambda$. Frenkiel and Klebanoff[9] obtained a unique curve which departed increasingly with increasing values of $n(n-1)\log_{10}R_\lambda$ from a straight line corresponding to a constant $\mu$. They concluded that their data were not therefore consistent with a constant value of $\mu$, at least in the context of the assumed log-normality of $(\partial u/\partial t)^2$. The validity of this conclusion cannot, however, be easily ascertained, in view of the inapplicability of Eq. (1) when $r = \eta$ and because of the observed departure of $(\partial u/\partial t)^2$ from the log-normal behavior.

Equations (1) and (5) can be combined to yield a relation of the form

$$F^n \propto (L/r)^{\mu_n} \tag{7}$$

with

$$\mu_n = n(n-1)\mu/2 \tag{8}$$

when $p(\chi_r)$ is log-normal. Using very general arguments of scale similarity,[10] Novikov also arrived at a relation similar to Eq. (7), but with the constraint that $\mu_n \leq \mu + n - 2$ for $n > 2$. Obviously, this bound is inconsistent with prediction (8) of the third hypothesis.

Figure 7 shows that, for a given $n$, $F^n$ follows Eq. (7) closely over a relatively wide range of $r/L$. The exponent $\mu_n$ is, however, lower than the log-normal value, with the deviation becoming more pronounced as $n$ increases (see Table II). They are consistent with the bounds given by Novikov and are in good agreement with those obtained by Kholmyanskii[11] who considered moments $\overline{(\partial u/\partial t)^{2n}}$ in the atmospheric surface layer. Although there is no *a priori* reason to assume that the value of $\mu$ is the same for scalar and velocity fields,

the bounds on $\mu_n$ as given by Novikov would apply irrespective of the field used. Somewhat surprisingly, both Kholmyanskii's and the present values of $\mu_n$ are in good agreement with Novikov's[7] result

$$\mu_n = n - \log_2(n+1) \tag{9}$$

at least for $n > 3$. [For $n = 2$, Eq. (9) yields $\mu_2 = \mu = 0.41$, which is slightly larger than the present value.] Novikov obtained Eq. (9) by applying ale similarity arguments[7] to the breakdown coefficient associated with any non-negative field $y$ (the breakdown coefficient is defined as the ratio of values of $y$ averaged over different length scales within the scale similarity range) and by choosing a rather simple form for the probability density of this coefficient.

## CONCLUSIONS

It appears that the probability density of $\ln\chi_r$ is close to normal even at a relatively small Reynolds number. However, higher order moments of $\chi_r$ are significantly lower than the values implied by the use of Kolmogoroff's third hypothesis. This does not appear to be a limitation of the Reynolds number of the flow, since Kholmyanskii's results obtained for one component of $\epsilon_r$ in the atmosphere are also similar. In fact, Novikov's bounds on $\mu_n$ suggest that $p(\chi_r)$ will never be close enough to log-normality to enable higher order moments to be calculable from Eq. (8).

## ACKNOWLEDGMENTS

The work described in this paper represents part of a program of research supported by the Australian Research Grants Committee.

[1]A. N. Kolmogoroff, J. Fluid Mech. **13**, 81 (1962).
[2]A. M. Obukhov, J. Fluid Mech. **13**, 77 (1962).
[3]A. M. Yaglom, Dokl. Akad. Nauk SSSR **166**, 49 (1966) [Sov. Phys.-Dokl. **11**, 26 (1966)].
[4]A. S. Gurvich and A. M. Yaglom, Phys. Fluids Suppl. **10**, 59 (1967).
[5]K. R. Sreenivasan, R. A. Antonia, and H. Q. Danh, Phys. Fluids 20, (1977).
[6]C. H. Gibson and P. J. Masiello, *Statistical Models and Turbulence*, edited by M. Rosenblatt and C. W. Van Atta (Springer-Verlag, Berlin, 1971), p. 427.
[7]E. A. Novikov, Prikl. Mat. Mekh. 35, 266 (1971) [J. Appl. Math. Mech. 35, 231 (1971)].
[8]C. H. Gibson, C. A. Friehe, and S. O. McConnell, Phys. Fluids **20**, S156 (October, Part II, 1977).
[9]F. N. Frenkiel and P. S. Klebanoff, Boundary Layer Meteorol. 8, 173 (1975).
[10]A. S. Monin and A. M. Yaglom, in *Statistical Fluid Mechanics*, edited by J. Lumley (The M. I. T. Press, Cambridge, 1975), Vol. 2, p. 615.
[11]M. Z. Kholmyanskii, Izv. Acad. Sci. USSR Atmos. Oceanic Phys. 8, 818 (1972).